MOLECULAR PHYSICS, 1997, VOL. 91, NO. 6, 977–992

Intermolecular relaxation involving coupled spin systems: a simplified approach to solvent induced relaxation

By N. R. SKRYNNIKOV†§, T. N. KHAZANOVICH‡
and B. C. SANCTUARY†

† Chemistry Department, McGill University, Montreal, Quebec, Canada H3A 2K6
‡ N. N. Semenov Institute of Chemical Physics, Moscow, 117334, Russia

(*Received 23 May 1996; revised version accepted 5 November 1996*)

Intermolecular dipole–dipolar relaxation is considered in the framework of Redfield equations describing the evolution of the spin density matrices for multicomponent solutions. Two types of contribution from intermolecular dipole–dipolar interactions are identified. Contributions of the first type can be emulated using the external random field (ERF) model, while contributions of the second type cannot. The latter are responsible for relaxation coupling between solute and solvent, and can be expressed in terms of cross-relaxation rates. A complete system of Redfield equations for multicomponent liquids is not practical due to its size and the multitude of unknown parameters. For this reason, interpretation of experimental data usually is limited to the ERF model, even if unreliable for experiments where solvent spins are exposed to the effect of pulses. As an alternative, it has been suggested that complete system of Redfield equations can be truncated so that the solvent part is limited to spin polarizations. Solvent multispin modes are ignored as insignificant from the point of view of solute relaxation. So formulated, this approach is referred to as the 'coupled solute solvent relaxation' (CSSR) model. The validity of this approximation is examined using the examples of AX–AB and AX–ABX type binary mixtures. The elements of complete Redfield matrices embracing both solute and solvent are calculated. The results include cross-correlations between intermolecular dipolar interactions, which are calculated for spherical molecules with off-centre spin sites. Simulations indicate that the CSSR approach provides a very accurate approximation, regardless of the inherently complex nature of solvent relaxation and the existence of several potential paths for intermolecular magnetization transfer. It offers improvement over the ERF model, particularly in the evaluation of intermolecular contributions, in the case when both solute and solvent spins come under the effect of RF pulses during the course of experiments.

1. Introduction

Sophisticated experimental techniques based on a variety of relaxation effects have become instrumental in the investigation of complex molecular systems in solutions. Two aspects should be emphasized. First, intensive use is made of the long-range NOE, including intermolecular magnetization transfer [1–3]. This underscores the importance of long-range dipole–dipolar interaction which serves as a unique probe for the investigation of molecular dynamics and structure, in particular for large biomolecules. Second, the studies of multimode (coupled) relaxation are increasingly popular [4, 5]. Multimode relaxation, involving multispin orders and coherences that appear in coupled spin systems [6], complements T_1 and T_2 measurements, providing additional information on molecular structure and motion.

As involved as it is, the theory of multimode relaxation tends to avoid further complications arising from intermolecular paths. Instead, the intermolecular dipole–dipolar (DD) interaction usually is modelled by an external random field (ERF) fictitious first-order spin Hamiltonian. The pitfalls of this model are known [7, 8] but the belief exists that ERF provides a reasonable approximation when applied with a due caution.

At the same time, the theory that incorporates DD interactions between coupled spin systems in multicomponent solutions has been developed [7, 9]. Solomon's equations for the intermolecular relaxation of spins 1/2 give a simple example of such a treatment [10, 11]. The generalized formalism puts together the concept of multimode relaxation and the theory of translational correlation functions [12–16]. The results potentially contain more information on solute–solvent interactions, since the analysis deals with coupled spin systems rather than single-spin molecules. Rich spin context provides access

§ Present address: Laboratorium für Physikalische Chemie, ETH Zentrum, 8092 Zürich, Switzerland.

to fine details of molecular dynamics, such as roto-translational cross-correlation functions [7] discussed in what follows. At the same time, the interpretation of traditional experiments on coupled relaxation is improved, since external relaxation is accounted for accurately in this approach.

While generalized theory of intermolecular relaxation is available, the examples of its application are rare, and this is not accidental. The analysis employing a complete set of spin density matrices faces serious challenges. One is the large number of relaxation coefficients, and the size of the ensuing equations. Another problem is the large number of dynamic and structural parameters involved. Thus, it is desirable to find a simplified description, more compact than a full system of Redfield equations for a multicomponent solution, yet more precise than a reduced system relying on the ERF model.

Such a description has been introduced by two of us under the name 'coupled solute solvent relaxation' (CSSR) [17]. Similar to the ERF model, it focuses on one particular spin system, conventionally that of the solute (assuming that the details of solvent relaxation are of no interest), and is only slightly more difficult technically. In essence, the CSSR approach assumes that solvent can be represented by a single spin polarization, regardless of how complex is the composition of its spin system.

So far the CSSR model has been introduced *ad hoc*, with no appropriate substantiation. Such a substantiation certainly is needed, since in this approach we ignore the complex character of solvent relaxation, and even part of magnetization transfer between solute and solvent. In the present paper we intend to show that CSSR approximation describes intermolecular DD relaxation adequately.

A good example is provided by the NMR studies of small molecules dissolved in liquid crystals [18]. Intermolecular DD interactions provide important relaxation mechanism in such systems. Consequently, the question arises as to how to take the intermolecular relaxation into account. An attempt to construct a full-scale system of Redfield equations, embracing dozens of coupled protons in a liquid crystal, seems counterproductive. On the other hand, the ERF model is less than perfect (in particular, it runs into difficulties interpreting intermolecular relaxation rates obtained for hydrogenated liquid crystals versus deuterated [19–22]). In these circumstances, CSSR seems to be a possible answer to the problem. In this approach, a single effective relaxation rate is assigned to the liquid crystal ^{1}H (selective investigation of the proton relaxation is impossible since the spectra of liquid crystals are broadened). It also utilizes intermolecular NOEs, that can be measured directly and allow for the model interpretation [23–25].

In section 2 we consider a complete system of Redfield equations for a multicomponent mixture as presented in the operator basis (in Liouville space). It is shown that certain intermolecular contributions can be emulated within a framework of the ERF model. The remaining intermolecular contributions, that cannot be reproduced using the ERF Hamiltonian, represent relaxation coupling between solute and solvent. Such coupling is possible only between those solute and solvent modes that contain a one-spin part. This rigorous result clarifies the scope and the structure of intermolecular coupling in a full relaxation matrix.

The CSSR approximation can be put to a most thorough test by examining the systems that contain tightly coupled solvent spins. Section 3 describes full relaxation matrices for AX-AB and AX-ABX type mixtures, with an eye on the elements that are neglected in the CSSR approximation. Evaluation of the Redfield matrix requires knowledge of roto-translational cross-correlation functions. These are calculated in section 4 based on a simple model of spherical molecules with off-centre spin sites. Section 5 compares solute relaxation curves produced on the basis of full Redfield matrices and truncated CSSR and ERF type matrices, so that the accuracy of the CSSR approximation can be judged.

2. Equations of multimode spin–lattice relaxation in mixtures

With the increasing sophistication of relaxation experiments, a variety of auto- and cross-correlation contributions have been brought to the attention of researchers. There is a tendency to believe that many more examples of unusual relaxation coupling and exotic cross-correlations can be found. Solutions of proteins may serve as an illustration for this point. It has been recognized [26] that protein folding and stability, as well as binding and catalytic functions, are determined largely by interactions with solvent water. It remains unclear, however, whether regular NOE represents the only channel for magnetization transfer from water to protein, or whether magnetization can also flow directly into two- or three-spin orders of protein. It further remains to be seen if such effects have any impact on the results of state-of-the-art experiments that measure relaxation of multispin modes throughout the polypeptide chain [27].

Under these circumstances, general consideration can be helpful in determining what sort of relaxation coupling is possible, or impossible, without going into details of a spin system. This type of analysis is carried out here for intermolecular DD interactions. In particular, it demonstrates that intermolecular relaxation can couple

only those solute and solvent modes that contain one-spin components, and the coupling comes from DD autocorrelations. It further helps to define the simplified approach to intermolecular relaxation.

Consider a multicomponent liquid in which one of the components is represented by N_χ molecules of the sort χ (different molecules of the same sort are denoted χ and $\tilde{\chi}$). Each of these molecules bears m_χ magnetic nuclei with spins 1/2. Consideration is limited to spins 1/2 since the relaxation of higher spins is dominated by the quadrupolar mechanism which dwarfs any intermolecular contribution. The static spin Hamiltonian for each of these molecules includes Zeeman and scalar coupling terms [28]. Corresponding Liouville space is spanned with basic operators Q_m^χ, that are normalized in standard fashion, $\mathrm{Tr}_\chi\{Q_m^{\chi\dagger} Q_n^\chi\} = \delta_{mn}$, where Tr_χ is the trace over spin space of a single molecule χ. The part of this basis relevant for spin–lattice relaxation consists of the modes commuting with the static spin Hamiltonian.

In existing theories [7–9, 29, 30], the spin density matrix of the entire system is represented as a direct product of molecular density matrices, which is reduced to the sum of the constituent density matrices by use of the high temperature approximation. This is tantamount to the assumption that intermolecular spin correlations can be neglected in the relaxation analyses of liquids [29, 31]. One known exception is intermolecular coherences induced by the dipolar field [32, 33]. This phenomenon has been attributed to the small (due to symmetry and molecular motion), yet observable, residual constant part of DD interaction. Jeener, Vlassenbroek and Broekaert [33] conclude that any resulting intermolecular correlations can be neglected in relaxation coefficients, and accounted for through a static Hamiltonian within the framework of standard Redfield theory. Our presentation does not address this special effect.

Based on these premises, the equation of motion for the spin density matrix is obtained including intermolecular effects. The analysis, carried out previously in a basis derived from the Hilbert space wavefunctions, can be reformulated conveniently in the operator basis embedded in the Liouville space. The equations describing spin–lattice relaxation in mixtures, and explicit results for relaxation coefficients originating from intermolecular dipole–dipolar interactions, are given in what follows.

The hypothesis of statistical independence of molecular spin systems in solution (equivalent to neglect of any intermolecular spin correlations) and the high temperature approximation reduce Liouville space [28] to the one spanned with operators $V_m^\chi = \sum^{N_\chi} Q_m^\chi$, where the sum is taken over all molecules of this particular sort, and Q_m^χ are (identical in form) operators, each referring to spins of one particular χ-sort molecule.

Non-equilibrium states of the spin system, developed over the course of a relaxation experiment, are characterized in full by a set of modes v_m^χ, obtained from V_m^χ by taking the trace over the spin density matrix. Since the spin density matrix of an entire system is given by a sum of molecular spin density matrices, v_m^χ can be expressed as:

$$v_m^\chi = N_\chi \frac{\mathrm{Tr}_\chi\{(\rho^\chi - \rho_{\mathrm{eq}}^\chi) Q_m^\chi\}}{\mathrm{Tr}_\chi\{\rho^\chi\}} = N_\chi \frac{\mathrm{Tr}_\chi\{(\rho^\chi - \rho_{\mathrm{eq}}^\chi) Q_m^\chi\}}{2^{m_\chi}}, \tag{1}$$

where ρ^χ and ρ_{eq}^χ are non-equilibrium and equilibrium spin density matrices of the molecule χ. The term 'magnetization modes' is normally associated with the expectation values, such as v_m^χ. Following Canet [34], we shall also employ this term for the components of the operator basis, such as Q_m^χ.

To this end, the master equation can be evaluated, giving rise to a system of coupled equations. For the purpose of our discussion it is sufficient to consider the binary mixture, comprising molecules of sort ζ and η (extension to multicomponent solutions is obvious).

$$\frac{\mathrm{d}}{\mathrm{d}t} v_m^\zeta = - R_{mk}^{(\zeta,\zeta)} v_k^\zeta - R_{ml}^{(\zeta,\eta)} v_l^\eta,$$

$$\frac{\mathrm{d}}{\mathrm{d}t} v_n^\eta = - R_{nk}^{(\eta,\zeta)} v_k^\zeta - R_{nl}^{(\eta,\eta)} v_l^\eta. \tag{2}$$

This is a generalization of Solomon's results for multimode relaxation in binary solutions. We plan to consider the relaxation coefficients $R_{mk}^{(\zeta,\zeta)}$ that couple spin modes belonging to the same molecule ζ, and $R_{ml}^{(\zeta,\eta)}$, responsible for the coupling between ζ and η modes.

The relaxation coefficient $R_{mk}^{(\zeta,\zeta)}$ contains an intramolecular contribution, along with intermolecular terms arising from the interaction between like and unlike molecules:

$$R_{mk}^{(\zeta,\zeta)} = \mathrm{Tr}_\zeta\{Q_m^{\zeta\dagger} \hat{\hat{R}}_\zeta^{\mathrm{intra}} Q_k^\zeta\} + N_\zeta \frac{\mathrm{Tr}_{\zeta\tilde{\zeta}}\{Q_m^{\zeta\dagger} \hat{\hat{R}}_{\zeta\tilde{\zeta}}^{\mathrm{inter}} (Q_k^\zeta + Q_k^{\tilde{\zeta}})\}}{2^{m_\zeta}} + N_\eta \frac{\mathrm{Tr}_{\zeta\eta}\{Q_m^{\zeta\dagger} \hat{\hat{R}}_{\zeta\eta}^{\mathrm{inter}} Q_k^\zeta\}}{2^{m_\eta}}. \tag{3}$$

Here $\hat{\hat{R}}_{\zeta\tilde{\zeta}}^{\mathrm{inter}}$ represents the Redfield superoperator for intermolecular relaxation of like molecules, where different molecules of the same sort are denoted as ζ and $\tilde{\zeta}$. Formal notation of $\hat{\hat{R}}_{\zeta\tilde{\zeta}}^{\mathrm{inter}}$ implies lattice average and double commutator over spin variables, and $\mathrm{Tr}_{\zeta\tilde{\zeta}}$ is equivalent to $\mathrm{Tr}_\zeta \mathrm{Tr}_{\tilde{\zeta}}$. Similarly $\hat{\hat{R}}_{\zeta\eta}^{\mathrm{inter}}$ represents relaxation of ζ by molecules of the different sort η, and $\hat{\hat{R}}_\zeta^{\mathrm{intra}}$

symbolizes intramolecular relaxation. This latter has been studied in great detail (see [5] and [34] for review) and will not be discussed here. Further discussion is focused on intermolecular terms.

Relaxation coefficients involve spectral densities of time-dependent correlation functions evaluated at eigenfrequencies determined by the static spin Hamiltonian. The combinations of Larmor frequencies are retained in the argument of spectral densities. Small shifts, such as chemical and scalar coupling shifts, can be dropped, since correlation times of molecular motion in liquids typically are small enough to satisfy $(\omega_i - \omega_{i'})\tau_c \ll 1$.

Definitions of spectral densities appearing in the literature differ by a constant factor. The one that is used here is

$$J_m^{is,i's'}(\omega) = \tfrac{1}{2}\int_{-\infty}^{\infty} e^{-i\omega t} g_m^{is,i's'}(t)\,dt, \qquad (4)$$

where i, i' label spins belonging to one molecule, s, s' label those belonging to the other molecule, and $g_m^{is,i's'}(t)$ is a correlation function for intermolecular dipole–dipolar interactions.

$$g_m^{is,i's'}(t) = \iint d\mathbf{r}_{is}\, d\mathbf{r}_{i's'} \mathcal{D}_{0m}^{(2)*}(\Omega_{is}) \mathcal{D}_{0m}^{(2)}(\Omega_{i's'}) \times P(\mathbf{r}_{is}, t|\mathbf{r}_{i's'}) f_0(\mathbf{r}_{i's'})/r_{is}^3 r_{i's'}^3. \qquad (5)$$

The conditional probability $P(\mathbf{r}_{is}, t|\mathbf{r}_{i's'})$ and the pair distribution function $f_0(\mathbf{r}_{i's'})$ are the same as described by Hwang and Freed [12].

Using a spherical tensor representation for the dipole–dipolar Hamiltonian and a Liouville space formulation of the Redfield theory [28], one can compute the last term in equation (3), obtaining

$$2^{-m_\eta} N_\eta \mathrm{Tr}_{\zeta\eta}\{Q_m^{\zeta\dagger} \hat{\hat{R}}_{\zeta\eta}^{\mathrm{inter}} Q_k^{\zeta}\} = \sum_{i}^{m_\zeta} \sum_{s}^{m_\eta} \tfrac{5}{4} D_{is} D_{i's} n_\eta \times \sum_{p}^{1} \sum_{q}^{1} \left\{ \begin{pmatrix} 1 & 1 & 2 \\ p & q & -(p+q) \end{pmatrix} \right\}^2 \times \mathrm{Tr}_\zeta\left\{ \left[I_{ip}^{(1)}, Q_m^{\zeta} \right] \left[Q_k^{\zeta}, I_{i'p}^{(1)\dagger} \right] \right\} J_{p+q}^{is,i's}(p\omega_i + q\omega_s), \qquad (6)$$

where the first summation is over all pairs of spins from molecule ζ, the second summation over all spins of molecule η, and the third over spherical components of the spin operator $I_{ip}^{(1)}$. Contributions from each pair of dipole–dipolar interactions include molecular density, $n_\eta = N_\eta/V$, dipolar interaction constants, $D_{is} = -\sqrt{6}(\mu_0/4\pi)\hbar\gamma_i\gamma_s$, and Wigner 3-j coefficients. The property of traceless spherical tensors

$$\mathrm{Tr}\left\{ I_{ip}^{(l)} \right\} = 0, \quad l > 0 \qquad (7)$$

has been used to compute Tr_η and arrive at the above results.

It is not difficult to verify that contribution (6) can be mimicked by use of an ERF Hamiltonian [28] in place of the dipole-dipolar Hamiltonian. With the relaxation superoperator $\hat{\hat{R}}_{\zeta\eta}^{\mathrm{inter}}$ based on the ERF Hamiltonian instead of DD the contribution (6) can be recomputed, yielding

$$2^{-m_\eta} N_\eta \mathrm{Tr}_{\zeta\eta}\{Q_m^{\zeta\dagger} \hat{\hat{R}}_{\zeta\eta}^{\mathrm{inter}} Q_k^{\zeta}\} = \sum_{i,i'}^{m_\zeta} \gamma_i \gamma_{i'} \sum_{p}^{1} \mathrm{Tr}_\zeta\left\{ \left[I_{ip}^{(1)}, Q_m^{\zeta} \right] \left[Q_k^{\zeta}, I_{i'p}^{(1)\dagger} \right] \right\} J_p^{i,i'}(p\omega_i). \qquad (8)$$

The new spectral density $J_p^{i,i'}(\omega)$ appearing here characterizes the time-dependent correlation between random fields at the sites of spins i and i':

$$J_m^{i,i'}(\omega) = \tfrac{1}{2}\int_{-\infty}^{\infty} e^{-i\omega t} \langle B_{im}^*(t) B_{i'm}(0) \rangle\, dt. \qquad (9)$$

In this expression B_{im} are spherical components of the random field vector, reflecting the net effect of spins s on spin i.

Equations (8) and (9) can be compared with the results obtained previously for DD relaxation and given in equations (4) and (6). Comparison reveals that all DD contributions are matched by the ERF contributions. Moreover, they can be equated, leading to

$$\langle B_{ip}^*(t) B_{i'p}(0) \rangle = \sum_{s}^{m_\eta} \frac{15}{2} \left(\frac{\mu_0}{4\pi} \right)^2 \hbar^2 \gamma_s^2 n_\eta \times \sum_{q}^{1} \left\{ \begin{pmatrix} 1 & 1 & 2 \\ p & q & -(p+q) \end{pmatrix} \right\}^2 \times g_{p+q}^{is,i's}(t) e^{iq\omega_s t}. \qquad (10)$$

It is worth noting that this result quantifies the relation between ERF random fields and genuine intermolecular DD correlation functions. In summary, intermolecular contribution in $R_{mk}^{(\zeta,\zeta)}$ can be modelled successfully by use of the ERF. This conclusion is true equally for intermolecular interactions between like molecules, the second term in equation (3), as can be shown by similar calculations.

Next, let us consider relaxation coefficients $R_{ml}^{(\zeta,\eta)}$ corresponding to mutual relaxation of different species. At this point, note that Q_m^{ζ} can be represented as a linear combination of operator products $I_{ip}^{(1)} I_{i'q}^{(1)} \ldots$ (for example, see equations (14) and (16) below). Modes are

classified in n-quantum manfolds according to $p + q + \ldots$value.

Since the dipole–dipolar Hamiltonian is bilinear in spin operators, it follows from the definition of $R_{ml}^{(\zeta,\eta)}$ and property (7) that only one-spin and two-spin products give rise to non-zero relaxation coefficients. Three-spin, or higher, products contain spin operators $I_{ip}^{(1)}$ that cannot be matched by spin operators in the Hamiltonian, and therefore result in zero trace. By the same reasoning, first-rank relaxation mechanisms fail to contribute to $R_{ml}^{(\zeta,\eta)}$. Furthermore, the double commutator in $\hat{\hat{R}}_{\zeta\eta}^{\text{inter}}$ can be simplified using commutation relations:

$$\left[I_{ip}^{(1)}I_{i'q}^{(1)}, I_{ir}^{(1)}I_{i's}^{(1)}\right] = I_{ip}^{(1)}I_{ir}^{(1)}\left[I_{i'q}^{(1)}, I_{i's}^{(1)}\right] + \left[I_{ip}^{(1)}, I_{ir}^{(1)}\right]I_{i's}^{(1)}I_{i'q}^{(1)},$$

$$\left[I_{ip}^{(1)}, I_{iq}^{(1)}\right] = (-1)^{q+p}\sqrt{6}\begin{pmatrix} 1 & 1 & 1 \\ -(p+q) & q & p \end{pmatrix} I_{i,p+q}^{(1)}, \tag{11}$$

based on the usual momentum commutation rules. After simplification, it can be seen that only single-spin operators give rise to non-zero relaxation coefficients, and this is due to intermolecular DD autocorrelation. All other remaining possibilities are ruled out by the same argument that the presence of a lone spin operator results in zero trace (equation (7)). The only non-zero contribution comes from the intermolecular DD mechanism:

$$R_{ml}^{(\zeta,\eta)} = 2^{-m_\zeta} N_\zeta \mathrm{Tr}_{\zeta\eta}\{Q_m^{\zeta\dagger}\hat{\hat{R}}_{\zeta\eta}^{\text{inter}}Q_l^{\eta}\}, \tag{12}$$

and this is different from zero iff both Q_m^{ζ} and Q_l^{η} include single-spin operators. In view of these observations, $R_{ml}^{(\zeta,\eta)}$ is nothing other than a linear combination of standard DD cross-relaxation rates:

$$C = \tfrac{1}{12}D_{is}^2(6J_2^{is,is}(\omega_i + \omega_s) - J_0^{is,is}(\omega_i - \omega_s)). \tag{13}$$

Finally, according to the preceding discussion, these relaxation coefficients *cannot* be reproduced by use of the ERF model since the latter is based on the first-rank Hamiltonian. This is a manifestation of the main shortcoming of the ERF model: its failure to reproduce the intermolecular NOE.

General results presented here will be applied to specific spin systems in the following sections.

3. Relaxation in AX–AB and AX–ABX mixtures

A general framework for treating spin–lattice relaxation in mixtures is presented above. However, in experimental practice, a compact formulation accounting for solvent induced relaxation is desirable. As shown above, direct relaxation coupling between solute and solvent occurs only in the context of one-spin operators. This suggests that of all solvent modes Q_k^{η} only single-spin polarizations are important for solute relaxation (the hypothesis, introduced under the name of CSSR).

The CSSR approach is aimed primarily at complex solvents, such as liquid crystalline solvents. The exact treatment does not seem feasible in this case due to the size of the solvent spin system and the multitude of structural and dynamic parameters, such as spin coordinates and correlation times of local motions. Even for relatively simple solvents, that can be treated using the exact theory, the CSSR approach proves useful since it allows us to focus on solute relaxation and avoid tedious measurements of solvent relaxation (the details of solvent relaxation usually are of little interest).

Before the CSSR approach can be used in practice, it has to be tested, since so far there is no reason to believe that it would provide for the satisfactory approximation (except for the intuitive insight). In fact, it has not even been confirmed that the CSSR offers an improvement over the ERF model. The only way of verifying that is by investigating simple model systems that lend themselves for the exact treatment.

Pursuing this strategy, we examine two simple binary mixtures, with solute represented by AX and solvent by AB or ABX spin systems. The relaxation behaviour of the solute is at the centre of the study. The notations ab, abx are adopted for solvent in what follows in order to discriminate between spins in solute and solvent, thus eliminating the need for a molecular label ζ. In calculation of relaxation rates A and a are treated as spins of different sorts, as well as X and x. As an argument of spectral density ω_a and ω_b are interchangeable according to the remark made in section 2. Operator modes pertaining to spin–lattice relaxation in AX–ab are

$$Q_1 = I_{Az}, \qquad Q_2 = I_{Xz}, \qquad Q_3 = 2I_{Az}I_{Xz}$$

$$Q_4 = \tfrac{1}{\sqrt{2}}(I_{az} + I_{bz}), \qquad Q_5 = 2I_{az}I_{bz},$$

$$Q_6 = \tfrac{1}{\sqrt{2}}(\cos\phi(I_{az} - I_{bz}) + \sin\phi(I_{a+}I_{b-} + I_{a-}I_{b+})), \tag{14}$$

where ϕ is a strong coupling parameter for the ab system, $\tan\phi = J_{ab}/(\omega_a - \omega_b)$.

In the CSSR approach, only the total spin polarization Q_4 is retained of three ab modes, the assumption being tantamount to the equivalence of a and b spins. The question remains if a and b can be treated as equivalent, without compromising the analysis of AX relaxation.

The calculation of spin–lattice relaxation coefficients (equations (3), (12)) has been performed in full, including intermolecular relaxation of like molecules, without making any assumptions regarding relative concentrations of the components. The result for the

Table 1. Relaxation matrix elements for spin–lattice relaxation in an AB liquid: contributions from intermolecular DD interactions. Complete expressions for R_{ij} are obtained by multiplication of all entries by a factor n_2, where n_2 is the concentration of the ab species, and summation through the respective rows. Only non-zero elements, $R_{ij}\, j \geqslant i$, are listed in view of the $R_{ij} = R_{ji}$ symmetry. The notations are explained in the text (equations (13) and (15)).

	$H_{\mathrm{DD}}^{\mathrm{a\alpha}} - H_{\mathrm{DD}}^{\mathrm{a\alpha}}$	$H_{\mathrm{DD}}^{\mathrm{b\beta}} - H_{\mathrm{DD}}^{\mathrm{b\beta}}$	$H_{\mathrm{DD}}^{\mathrm{a\beta}} - H_{\mathrm{DD}}^{\mathrm{a\beta}}$	$H_{\mathrm{DD}}^{\mathrm{a\alpha}} - H_{\mathrm{DD}}^{\mathrm{b\alpha}}$	$H_{\mathrm{DD}}^{\mathrm{a\beta}} - H_{\mathrm{DD}}^{\mathrm{b\beta}}$
R_{44}	$\frac{1}{2}(T + C)$	$\frac{1}{2}(T + C)$	$T + C$		
R_{46}	$\frac{1}{2}\cos\phi(T + C)$	$-\frac{1}{2}\cos\phi(T + C)$			
R_{55}	T	T	$2T$		
R_{56}				$-\sqrt{2}\sin\phi\, T$	$-\sqrt{2}\sin\phi\, T$
R_{66}	$\frac{1}{2}(T + \cos^2\phi\, C + \sin^2\phi\, P)$	$\frac{1}{2}(T + \cos^2\phi\, C + \sin^2\phi\, P)$	$T - \cos^2\phi\, C + \sin^2\phi\, P$	$-\sin^2\phi\, P$	$-\sin^2\phi\, P$

Table 2. Relaxation matrix elements for spin–lattice relaxation in an AX–ab mixture: contributions from intermolecular DD interactions between AX and ab. Intermolecular interactions involving spin X are excluded. Only non-zero elements, $R_{ij}\, j \geqslant i$, are listed. Off-diagonal elements that couple AX and ab blocks are related by $R_{41} = (n_2/n_1)R_{14}$, $R_{61} = (n_2/n_1)R_{16}$, and the rest of the matrix displays $R_{ij} = R_{ji}$ symmetry.

	$H_{\mathrm{DD}}^{\mathrm{Aa}} - H_{\mathrm{DD}}^{\mathrm{Aa}}$	$H_{\mathrm{DD}}^{\mathrm{Ab}} - H_{\mathrm{DD}}^{\mathrm{Ab}}$	
R_{11}	$n_2 T$	$n_2 T$	
R_{14}	$n_1 \frac{1}{\sqrt{2}} C$	$n_1 \frac{1}{\sqrt{2}} C$	
R_{16}	$n_1 \frac{1}{\sqrt{2}} \cos\phi\, C$	$-n_1 \frac{1}{\sqrt{2}} \cos\phi\, C$	
R_{33}	$n_2 T$	$n_2 T$	
	$H_{\mathrm{DD}}^{\mathrm{aA}} - H_{\mathrm{DD}}^{\mathrm{aA}}$	$H_{\mathrm{DD}}^{\mathrm{bA}} - H_{\mathrm{DD}}^{\mathrm{bA}}$	$H_{\mathrm{DD}}^{\mathrm{aA}} - H_{\mathrm{DD}}^{\mathrm{bA}}$
R_{44}	$n_1 \frac{1}{2} T$	$n_1 \frac{1}{2} T$	
R_{46}	$n_1 \frac{1}{2} \cos\phi\, T$	$-n_1 \frac{1}{2} \cos\phi\, T$	
R_{55}	$n_1 T$	$n_1 T$	
R_{56}			$-n_1 \sqrt{2} \sin\phi\, T$
R_{66}	$n_1 \frac{1}{2}(T + \sin^2\phi\, P)$	$n_1 \frac{1}{2}(T + \sin^2\phi\, P)$	$-n_1 \sin^2\phi\, P$

intermolecular relaxation of ab molecules and the intermolecular relaxation between AX and ab species are tabulated below. The relaxation coefficients are expressed in terms of standard combinations of spectral densities. The combinations arising from DD interactions between spins i and s, and i' and s' (where i' and s' may or may not refer to the same spins as i and s), $H_{\mathrm{DD}}^{is} - H_{\mathrm{DD}}^{i's'}$, are:

$$T = \tfrac{1}{12} D_{is} D_{i's'} \left(J_0^{is,i's'}(\omega_i - \omega_s) + 3J_1^{is,i's'}(\omega_i) + 6J_2^{is,i's'}(\omega_i + \omega_s) \right),$$

$$P = \tfrac{1}{12} D_{is} D_{i's'} \left(4J_0^{is,i's'}(0) + 6J_1^{is,i's'}(\omega_s) \right), \qquad (15)$$

plus cross-relaxation rate C, quoted in equation (13). Note that the order of spin labels in $H_{\mathrm{DD}}^{is} - H_{\mathrm{DD}}^{i's'}$, as they appear in tables 1 and 2, is meaningful: it determines frequencies in T and P in accordance with the above convention. Mirror pairs of cross-correlations, $H_{\mathrm{DD}}^{is} - H_{\mathrm{DD}}^{i's}$ and $H_{\mathrm{DD}}^{i's} - H_{\mathrm{DD}}^{is}$, are summed up and placed in one column, with no distinction made between ω_{a} and ω_{b} in the argument of spectral densities. Intermolecular interactions involving spin X are omitted from table 2, but their contribution can be recovered by noting that operator modes (14) are symmetrical with respect to A and X. It is common to ignore this contribution when X is identified with ^{13}C or ^{15}N. The results for ab relaxation are in agreement with previous calculations by Khazanovich and Zitserman [7] in the extreme narrowing limit, except for the sign of R_{16}.

A remarkable feature is the appearance of intermolecular DD cross-correlations [7, 35] in tables 1 and 2 (in the final columns). They appear here in the context of one-spin and two-spin orders unlike familiar intramolecular DD cross-correlations in weakly coupled

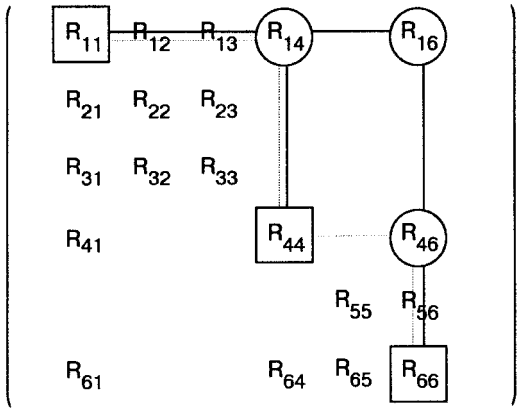

Figure 1. Structure of the relaxation matrix for an AX-ab mixture, including intramolecular DD interactions, intermolecular DD interactions between both like and unlike molecules (except those involving spin X), and CSA interactions for spins A and X. One-step (——) and two-step (••••••) magnetization transfer from the solvent spin system to the solute are shown.

systems that manifest themselves through three-spin orders. Intermolecular cross-correlation functions are expected to exist due to spatial correlation in the motion of spins a and b involved in DD interaction with given external spin. These quantities provide us with the refined measure for what has been referred to as 'cross-correlation of external random fields' and has been investigated within the scope of ERF model [19, 20]. The possibility of pursuing the effects of intermolecular DD cross-correlations in experiments over pure AB liquids has been pointed out by Vold and Vold [35].

By applying the CSSR approach to the system in question the complete composite basis (14) is reduced to Q_1–Q_4 modes. In doing so, we neglect the relaxation transfer through R_{16} and R_{46} (see figure 1). The former is due entirely to intermolecular DD interactions, as demonstrated in section 2, while the latter also may involve contributions from first-rank mechanisms. Of the two, only R_{16} affects AX spin system directly.

As seen from table 2, the magnitude of R_{16} is determined by differences in the Aa and Ab dipolar relaxation that can be attributed to inequivalent locations of a and b spins within a molecule. In the case when a and b are topologically equivalent R_{16} becomes zero, and the same is true for the dipolar part of R_{46}. By topological equivalence we mean that molecule allows for the symmetry operation that translates a into b (two spins still have different chemical shifts due to isotopic substitution, e.g., one is attached to ^{13}C, and the other to ^{12}C). While little can be done about R_{16}, the magnitude of R_{46} can be boosted by adding a third spin to the ab system. This third spin, x, placed in the proximity of a and well removed from b, produces a tangible difference in a and b relaxation that results in enhanced R_{46} transfer. This sort of qualitative reasoning led us to examine an abx (ABX) system in the role of solvent.

The abx spin modes that need to be added to Q_1 - Q_3 are as follows:

$$
\begin{aligned}
Q_4 &= \tfrac{1}{2}(I_{az} + I_{bz}), \quad Q_5 = \sqrt{2} I_{az} I_{bz}, \\
Q_6 &= \frac{1}{\sqrt{8}} (E_x + 2I_{xz})\{\cos \phi_+ (I_{az} - I_{bz}) \\
&\quad + \sin \phi_+ (I_{a+} I_{b-} + I_{a-} I_{b+})\}, \\
Q_7 &= \frac{1}{\sqrt{8}} (E_x - 2I_{xz})\{\cos \phi_- (I_{az} - I_{bz}) \\
&\quad + \sin \phi_- (I_{a+} I_{b-} + I_{a-} I_{b+})\}, \\
Q_8 &= \frac{1}{\sqrt{2}} I_{xz}, \quad Q_9 = (I_{az} + I_{bz}) I_{xz}, \\
Q_{10} &= \sqrt{8} I_{az} I_{bz} I_{xz}.
\end{aligned} \tag{16}
$$

where $\tan \phi_\pm = J_{ab}/(\omega_a - \omega_b \pm 1/2(J_{ax} - J_{bx}))$, and E_x is the spin x operator identity. Analogous to the ab mode Q_6 are modes Q_6 and Q_7, that correspond to orientation of x up and down respectively ($E_x \pm 2I_{xz}$ is equivalent to projection $2|\pm\rangle\langle\pm|_x$). In practice, simple product operators can be employed to generate relaxation coefficients. Subsequently, linear transformation can be used to form the relaxation matrix in the appropriate basis Q_1–Q_{10}.

Of all relaxation terms only intermolecular AX–abx relaxation is detailed here. Complete expressions for relaxation coefficients, including the intramolecular part, can be found on the World Wide Web site at http://bcs.chem.mcgill.ca/~nikolai. As discussed above, the coupling between spin polarization Q_4 and multispin modes Q_6 and Q_7 is due to the difference in ax and bx relaxation rates and, additionally, to intramolecular DD cross-correlations. Substantial relaxation coupling in the solvent spin system provides more stringent conditions for testing the CSSR model.

Diagonal elements in the abx relaxation matrix match their counterparts in the ab matrix, as expected. At the same time, off-diagonal elements within the abx block differ by a numerical factor (tables 2 and 3). The reason is that v_4^{ab}, v_5^{ab}, and v_6^{ab} all correspond to the amounts of magnetization different from v_4^{abx}, v_5^{abx}, and v_6^{abx}, and therefore are connected through different R_{ij} elements. Cross-relaxation elements (12) render the matrix of relaxation coefficients asymmetric (see caption to tables 2 and 3). Simple linear transformation with a diagonal transformation matrix can be applied to equation (2) in order to symmetrize the relaxation matrix prior to a diagonalization routine.

Table 3. Relaxation matrix elements for spin–lattice relaxation in an AX–abx mixture: contributions from intermolecular DD interactions between AX and abx. Intermolecular interactions involving spins X and x are excluded. Only non-zero elements, R_{ij} $j \geqslant i$, are listed. Off-diagonal elements that couple AX and abx blocks are related by $R_{41} = \frac{1}{2}(n_2/n_1)R_{14}$, $R_{61} = \frac{1}{2}(n_2/n_1)R_{16}$, $R_{71} = \frac{1}{2}(n_2/n_1)R_{17}$, where the factor of 1/2 is due to different dimensionality of the two spin systems. The rest of the matrix possesses symmetry.

	$H_{DD}^{Aa} - H_{DD}^{Aa}$	$H_{DD}^{Ab} - H_{DD}^{Ab}$	
R_{11}	$n_2 T$	$n_2 T$	
R_{14}	$n_1 C$	$n_1 C$	
R_{16}	$n_1 \frac{1}{\sqrt{2}} \cos\phi_+ C$	$-n_1 \frac{1}{\sqrt{2}} \cos\phi_+ C$	
R_{17}	$n_1 \frac{1}{\sqrt{2}} \cos\phi_- C$	$-n_1 \frac{1}{\sqrt{2}} \cos\phi_- C$	
R_{33}	$n_2 T$	$n_2 T$	
	$H_{DD}^{aA} - H_{DD}^{aA}$	$H_{DD}^{bA} - H_{DD}^{bA}$	$H_{DD}^{aA} - H_{DD}^{bA}$
R_{44}	$n_1 \frac{1}{2} T$	$n_1 \frac{1}{2} T$	
R_{46}	$n_1 \frac{1}{2\sqrt{2}} \cos\phi_+ T$	$-n_1 \frac{1}{2\sqrt{2}} \cos\phi_+ T$	
R_{47}	$n_1 \frac{1}{2\sqrt{2}} \cos\phi_- T$	$-n_1 \frac{1}{2\sqrt{2}} \cos\phi_- T$	
R_{55}	$n_1 T$	$n_1 T$	
R_{56}			$-n_1 \sin\phi_+ T$
R_{57}			$-n_1 \sin\phi_- T$
R_{66}	$n_1 \frac{1}{2}(T + \sin^2\phi_+ P)$	$n_1 \frac{1}{2}(T + \sin^2\phi_+ P)$	$-n_1 \sin^2\phi_+ P$
R_{69}	$n_1 \frac{1}{2\sqrt{2}} \cos\phi_+ T$	$-n_1 \frac{1}{2\sqrt{2}} \cos\phi_+ T$	
R_{77}	$n_1 \frac{1}{2}(T + \sin^2\phi_- P)$	$n_1 \frac{1}{2}(T + \sin^2\phi_- P)$	$-n_1 \sin^2\phi_- P$
R_{79}	$-n_1 \frac{1}{2\sqrt{2}} \cos\phi_- T$	$n_1 \frac{1}{2\sqrt{2}} \cos\phi_- T$	
R_{99}	$n_1 \frac{1}{2} T$	$n_1 \frac{1}{2} T$	
$R_{10,10}$	$n_1 T$	$n_1 T$	

The results presented in this section can be used for computations after choosing the model to generate correlation functions (5). Most challenging is the calculation of roto-translational cross-correlations (final columns in tables 1–3) which must take into account inequivalent positions of spins in a molecule. The model allowing for analytical calculations consists of a system of spherical molecules with off-centre spin sites involved in Brownian translational and rotational diffusion [36]. The eccentricity parameters describing off-centre spin sites can be used to specify inequivalent locations for a, b, and x. Autocorrelation functions were calculated for this model by Ayant *et al.* [14] and their treatment can be extended to cross-correlations as described in the following section.

4. Calculations of intermolecular correlation functions

Intermolecular correlation functions for spins in off-centre position were investigated first by Hubbard [36] using a Taylor series expansion for $\mathcal{D}_{0m}^{(2)}(\Omega_r)/r^3$. Generalization to a cross-correlation function (equation (5)) was done by Khazanovich and Zitserman [7]. The theory of intermolecular relaxation has been improved since [12, 13], and a complete solution in a form of series has been found by Ayant *et al.* [14]. The derivation presented in the latter work is extended here for intermolecular cross-correlations. Autocorrelation functions can be obtained as a limiting case from our results.

The system under consideration consists of spherical molecules undergoing free rotational and translational

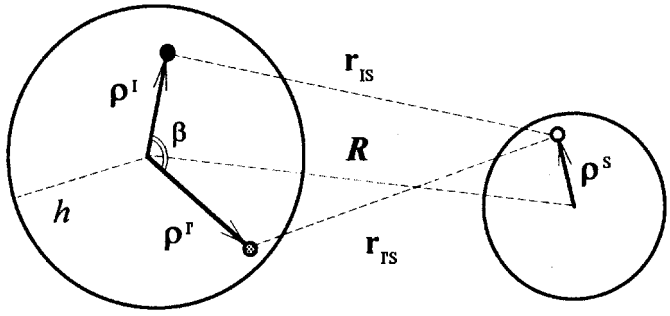

Figure 2. Schematic representation of the molecular geometry used in calculations of intermolecular DD cross-correlation functions.

diffusion, these two forms of motion are assumed to be independent. A hard sphere model pair distribution function is used. One of the molecules bears two spins, I and I', their sites specified by radial vectors ρ^I and $\rho^{I'}$ with the angle β between them. Both I and I' interact via the DD mechanism with the external spin S residing off-centre on the other molecule, its site being specified by ρ^S (figure 2). Due to the spherical symmetry of the problem the correlation function $g_m^{IS,I'S}(t)$ does not depend on the index m.

Following [14], it is convenient to introduce the vectors characterizing rotation in the molecular frame: $\rho^{IS} = \rho^I - \rho^S$, $\rho^{I'S} = \rho^{I'} - \rho^S$. Using a differential representation for spherical functions and invoking Legendre polynomials, one can perform the separation of rotational and translational variables in the correlation function.

$$g^{IS,I'S}(t) = 4\pi^2 \sum_{l,l'=0}^{\infty} \sum_{m=-l}^{l} \sum_{m'=-l'}^{l'} \times \frac{1}{(2l+1)(2l'+1)} G_{lm,l'm'} K_{lm,l'm'},$$

$$G_{lm,l'm'}(t) = \left\langle \frac{\partial^2}{\partial Z_0^2} \frac{Y^*_{l+2,m}(\mathbf{R}_0)}{R_0^{l+1}} \frac{\partial^2}{\partial Z^2} \frac{Y_{l'+2,m'}(\mathbf{R})}{R^{l'+1}} \right\rangle$$

$$K_{lm,l'm'}(t) = \langle [\rho_0^{IS}]^l Y_{l,m}(\rho_0^{IS}) [\rho^{I'S}]^{l'} Y^*_{l',m'}(\rho^{I'S}) \rangle. \qquad (17)$$

The quantities $[\rho^{IS}]^l Y_{l,m}(\rho^{IS})$ in the rotational correlator $K_{lm,l'm'}(t)$ obviously are transformed as spherical harmonics under rotations. On the other hand, the Hamiltonian of free Brownian diffusion is invariant under rotations of the coordinate system. Thus, the correlator $K_{lm,l'm'}(t)$ is non-zero only when $l = l'$, $m = m'$, and, in addition, does not depend on the value of m. The most detailed account of underlying symmetry considerations, that are in effect for all isotropic liquids, has been given by Hubbard [37]. The correlator $k_l(t) = K_{ll,ll}(t)$ can be calculated along the lines of [14] yielding

$$k_l(t) = 4\pi(2l+1)! \sum_{\lambda,\lambda'=0}^{l} \times \left[\frac{1}{(2\lambda+1)!(2\lambda'+1)!}\right]^{1/2} \times \left[\frac{1}{(2(l-\lambda)+1)!(2(l-\lambda')+1)!}\right]^{1/2} \times [\rho^I]^{\lambda} [\rho^{I'}]^{\lambda'} [\rho^S]^{2l-\lambda-\lambda'} \langle Y_{\lambda,\lambda}(\rho_0^I) Y^*_{\lambda',\lambda'}(\rho^{I'}) \rangle \times \langle Y_{l-\lambda,l-\lambda}(\rho_0^S) Y^*_{l-\lambda',l-\lambda'}(\rho^S) \rangle. \qquad (18)$$

The only difference here with the result obtained by Ayant *et al.* is the presence of $[\rho^I]^{\lambda}[\rho^{I'}]^{\lambda'}$ in place of $[\rho^I]^{\lambda+\lambda'}$ and of the cross-correlation function $\langle Y_{\lambda,\lambda}(\rho_0^I) Y^*_{\lambda',\lambda'}(\rho^{I'}) \rangle$ of molecular rotation in place of the corresponding autocorrelation function. Rotational cross-correlation functions for Brownian diffusion of the spherical top [11, 38] can now be used:

$$\langle Y_{\lambda,\lambda}(\rho_0^I) Y^*_{\lambda',\lambda'}(\rho^{I'}) \rangle = \delta_{\lambda,\lambda'} d_{00}^{(\lambda)}(\beta) \frac{1}{4\pi} \exp(-t/t_\lambda^I) = \delta_{\lambda,\lambda'} \frac{1}{4\pi} P_\lambda(\cos\beta) \exp(-t/t_\lambda^I),$$

$$\tau_\lambda^I = (\lambda(\lambda+1) D_{\mathrm{rot}}^I)^{-1}, \qquad (19)$$

where $P_\lambda(\cos\beta)$ is a Legendre polynomial, D_{rot}^I is the coefficient of rotational diffusion of the molecule containing I and I', and τ_2^I is further referred to as τ_{rot}^I. This renders $k_l(t)$ in its final form. It may be pointed out that rotational correlator (18) can be calculated for more elaborate types of motion, e.g., using the 'model-free approach' [39] for I and I' rotating around a slowly reorienting axis. The other correlator involved in equation (17), $G_{lm,l'm'}(t)$, describes purely translational correlation as associated with the intermolecular vector $\mathbf{R}$, and can be calculated along the lines of the general theory [12–14]. Finally, we summarize the expressions for the spectral density of the cross-correlation

function:

$$J_m^{IS,I'S}(\omega) = \frac{\pi}{30dD_{\text{transl}}^{IS}} \sum_{l=0}^{\infty} (2l+4)! \times \sum_{\lambda=0}^{l} \frac{1}{(2\lambda+1)!(2(l-\lambda)+1)!} \left[\frac{\rho^I}{d}\frac{\rho^{I'}}{d}\right]^{\lambda} \times P_\lambda(\cos\beta) \left[\frac{\rho^S}{d}\right]^{2(l-\lambda)} A_{l,\lambda}(\omega),$$

$$A_{l,\lambda}(\omega) = \text{Re}\left\{\frac{1}{z_{l,\lambda}^2}\left[\frac{1}{2l+3} - \frac{l+3}{z_{l,\lambda}^2} \times \left(1 + \frac{l+3}{z_{l,\lambda}} \frac{K_{l+5/2}(z_{l,\lambda})}{K_{l+3/2}(z_{l,\lambda})}\right)^{-1}\right]\right\},$$

$$z_{l,\lambda}(\omega) = \left[\tau_{\text{transl}}^{IS}\left(i\omega + \frac{1}{\tau_\lambda^I} + \frac{1}{\tau_{l-\lambda}^S}\right)\right]^{1/2} \quad (20)$$

where D_{transl}^{IS} is the coefficient of relative translational diffusion, $D_{\text{transl}}^{IS} = D_{\text{transl}}^{I} + D_{\text{transl}}^{S}$, $\tau_{\text{transl}}^{IS}$ is the corresponding correlation time, $\tau_{\text{transl}}^{IS} = d^2/D_{\text{transl}}^{IS}$, and d is the distance of closest approach equal to the sum of molecular radii, $d = h^I + h^S$.

A natural definition of eccentricity, $\varepsilon^I = \rho^I/h^I$, is used in consequent analyses. The distance d of the closest approach can be viewed as a fitting parameter absorbing the deficiencies of the model such as: absence of pair correlation effects, approximation of molecular shapes by spheres, etc. The functions $K_\upsilon(x)$ are expressed through the finite series [13]

$$K_\upsilon(x) = \left(\frac{\pi}{2x}\right)^{1/2} \times \exp(-x)\left(1 + \sum_{q=1}^{\upsilon-1/2} \frac{\prod_{p=1}^{q}(4\upsilon^2 - (2p-1)^2)}{q!(8x)^q}\right). \quad (21)$$

The autocorrelation function [14] is recovered automatically by taking $\beta = 0$, $\rho^I = \rho^{I'}$ in equation (20). It may be noted that the presence of $P_\lambda(\cos\beta)$ scales down the eccentricity effects and may eliminate them altogether, resulting in lower values of the spectral density than that corresponding to a central location of spins. It also modulates series in such a manner that vanishing terms can appear at any point, before the cut-off level is reached. The part of the series corresponding to the first three terms in l has been computed in reference [7] using Abragam's results [11] for translational correlation functions.

The dependence of the spectral density on the angle β is illustrated using the example of a hypothetical molecule with $\varepsilon^I = \varepsilon^{I'} = 0{\cdot}8$. For real molecules the angle β most often is small, but not necessarily so (for instance, $\beta = \pi$ for the pair of acetylene protons). As has been pointed out, the increase in β corresponds to the 'reversal' of eccentricity effects. Figure 3 shows that corrections become increasingly important with increase in $\omega\tau_{\text{transl}}$. This is in agreement with previous work [14], suggesting that eccentricity effects assume a greater role at higher frequencies. At low frequencies, the spectral density zooms in on extended time intervals, long enough for eccentricity effects to be averaged out by fast molecular rotation.

5. Exact and approximate approach to computations of relaxation curves

The examples of AX–ab and AX–abx solutions, considered in section 3, are now used to test the quality of the CSSR approximation. Both ab and abx solvents are represented by a single proton polarization Q_4 (equations (14) and (16)) in the CSSR approach. The relaxation coupling within the solvent spin system is therefore ignored, as well as direct solvent–solute coupling R_{16} (and R_{17} in case of abx). It is this solvent–solute coupling that will be discussed here first.

One useful parameter that helps to estimate the efficiency of R_{16} coupling can be formulated using a two by two matrix comprising R_{11}, R_{16}, R_{61}, and R_{66}. The extent of coupling can be analysed by evaluating the change in decay rates caused by R_{16}, and the degree of mixing between the two resulting exponentials. However, with two factors to be taken into account, this approach is ambiguous. Instead, a useful criterion can be borrowed from the theory of two-dimensional (2D) NOE experiments. We refer to a fictitious 2D NOE map corresponding to our two by two matrix, and estimate the maximum cross-peak amplitude as related to maximum amplitude of auto-peak, I_{16}/I_1 [40]. This approach has the advantage of being visualized easily and supplies us with a well defined measure for the transfer through R_{16}.

The analysis of transfer occurring within the two by two matrix can be carried out analytically [40] and an optimal mixing time can be determined for cross-peak buildup (maximum intensity of axial peak is simply $v_1(0)$). We summarize the resulting expressions below:

$$\mu_i^{[ij]} = I_{ij}/I_i = \frac{R_{ij}}{\lambda_-}\left(\frac{\lambda_-}{\lambda_+}\right)^{\frac{\lambda_+}{\lambda_+-\lambda_-}} \frac{v_j(0)}{v_i(0)},$$

$$\lambda_\pm = (1/2)\left\{(R_{ii}+R_{jj}) \pm \left[(R_{ii}-R_{jj})^2 + 4R_{ij}R_{ji}\right]^{1/2}\right\}, \quad (22)$$

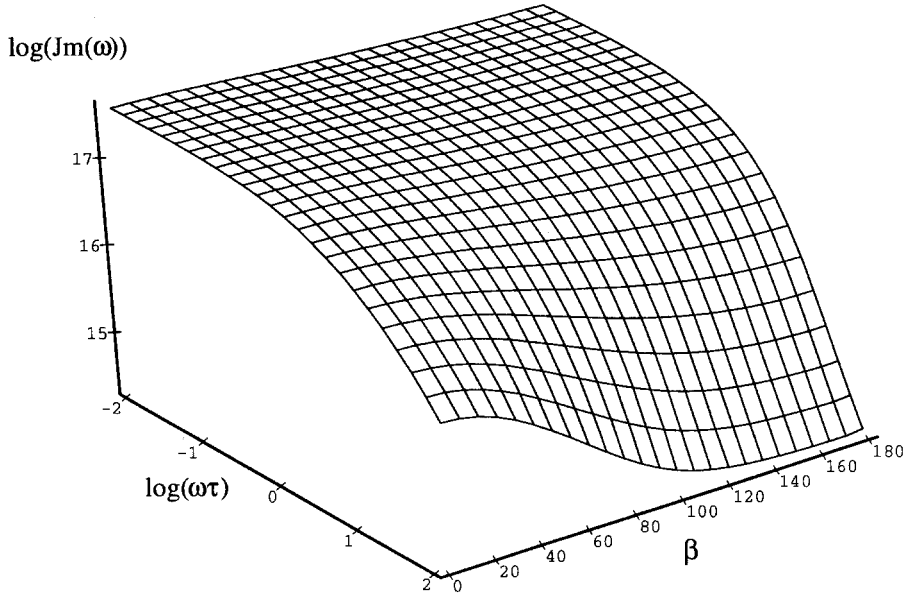

Figure 3. Spectral density of intermolecular DD cross-correlation $J_m^{IS,I'S}(\omega)$ (equation (20)) as a function of $\omega\tau_{\text{transl}}$ and the angle β. The surface is computed for the hypothetical fluid consisting of spherical molecules with 3 Å radius and spin eccentricities $\varepsilon^I = \varepsilon^{I'} = 0{\cdot}8$.

where $v_k(0)$ are initial conditions after the pulse (or preparation period) in relaxation measurements. The transfer is zero when the solvent spin system is unperturbed by RF pulses, $v_j(0) = 0$. This is in line with our general notion that relaxation in the system is affected only marginally by extraneous modes if these modes remain unperturbed.

We select further the parameters of the model system with the goal of testing the accuracy of the CSSR approximation under most unfavourable conditions, i.e., in the presence of significant R_{16} transfer. From an inspection of table 2 it is seen that maximum R_{16} transfer is expected in the weak coupling limit, $\phi = 0$ (conversely, R_{16} disappears in the limiting case of equivalent ab spins). This simple situation, when the solvent contains two weakly coupled or uncoupled protons, cross-relaxing each other, is handled here in the basis inherited from the ab system (equation (14)). This basis naturally includes the total solvent polarization, Q_4, that plays the key role in the CSSR approach.

The magnitude of R_{16} is determined by the difference in dipolar relaxation of A due to interaction with a and with b spins (table 2). With respect to the model described in section 4 this means that R_{16} is only non-zero when the eccentricities of spins a and b are significantly different. In order to increase R_{16}, spin eccentricities are set to $\varepsilon^a = 0{\cdot}8$, $\varepsilon^b = 0{\cdot}3$, corresponding to the large difference in eccentricities. The angle β is taken equal to zero so that eccentricity effects are not scaled down.

Our model allows for effective cross-relaxation between solvent spins a and b, as well as solute A and X. Chemical shift anisotropy (CSA) is added to both spins of AX in order to provide for differential relaxation [4]. All intermolecular dipolar interactions involving A, a, and b are taken into account.

This model has been used to simulate $v_1(t) - v_3(t)$ relaxation curves that fully characterize spin–lattice relaxation in an AX solute. The whole range of feasible dynamic parameters has been scanned in these simulations, covering extreme narrowing and slow motion limits. Rotational correlation times were varied from a small fraction of self-diffusion correlation times to their entire values. The mixture composition ranged from equimolar to dilute with respect to AX.

Two transfer coefficients $\mu_1^{[16]}$ and $\mu_1^{[14]}$ were determined, and four sets of $v_1(t) - v_3(t)$ curves were computed in each run: exact (obtained from full 6×6 relaxation matrix), CSSR (from truncated 4×4 matrix), ERF (from further truncated 3×3 matrix), and finally the one produced from a 3×3 matrix with no intermolecular contributions. The CSSR matrix contains the $\mu_1^{[14]}$ transfer path, but leaves $\mu_1^{[16]}$ outside, while the ERF matrix does not contain intermolecular NOE-type transfer at all. The results of the simulations show that transfer coefficients may indeed serve as good indicators for changes in relaxation curves. As $\mu_1^{[14]}$ approaches the level of several percentage points it brings about noticeable changes in the $v_1(t) - v_3(t)$ profiles, as illustrated by the difference in the CSSR and ERF curves (by noticeable we mean above the noise level, somewhat arbitrarily set at 5%).

Two families of relaxation curves, presented in figure 4, are obtained in the slow motion regime, $\omega\tau_{\text{transl}}^{\text{AXab}} = 100$, corresponding to a negative inter-

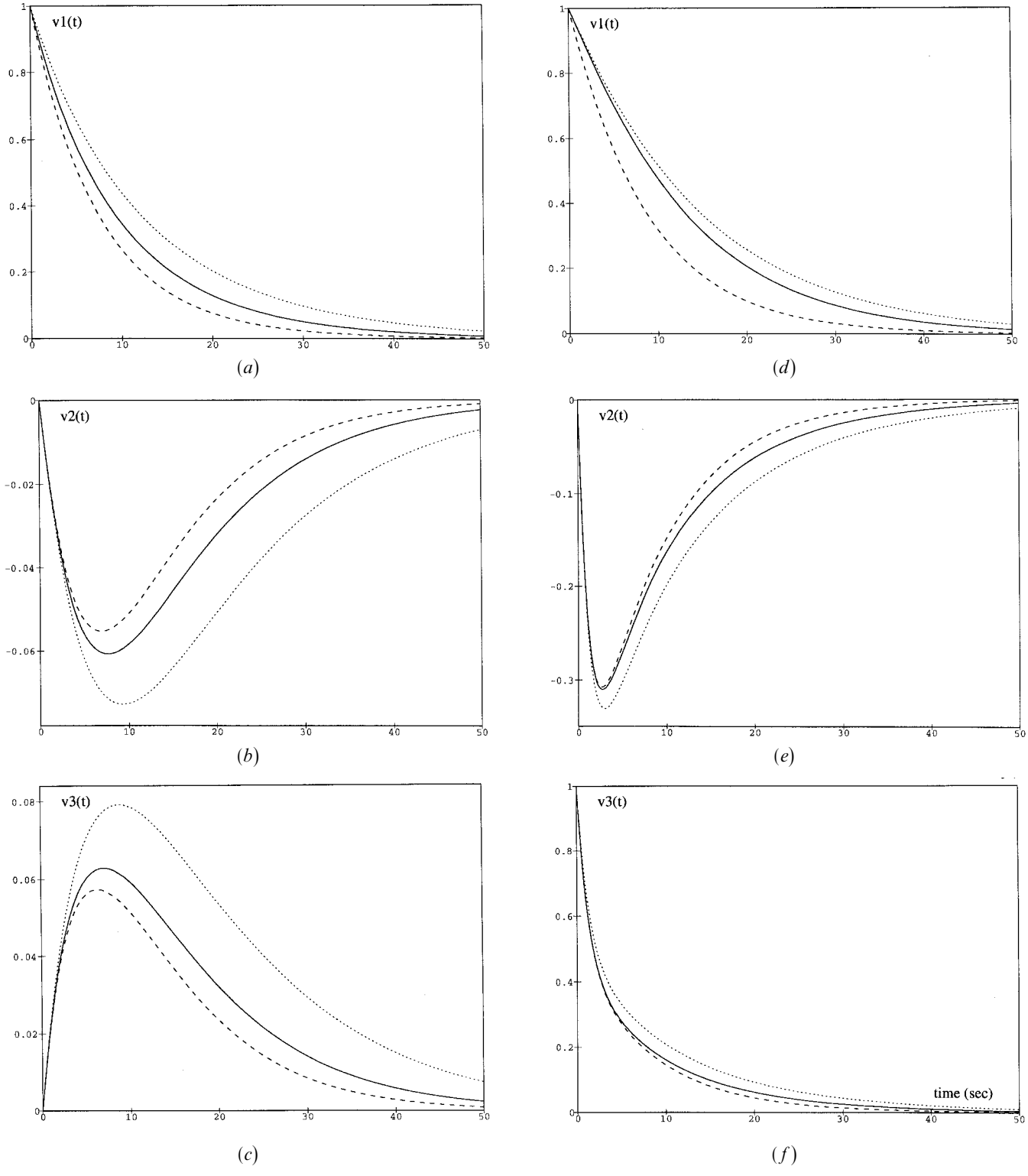

Figure 4. Relaxation profiles $v_1(t)$ - $v_3(t)$ (equations (1) and (14)) for an AX spin system interacting with an ab solvent. Scalar coupling in the ab system is vanishingly small. Initial conditions at time $t = 0$ include (*a–c*) non-selective inversion of A and (*d–f*) selective inversion of the low-field line in the A doublet. In both cases excitation is accompanied by nearly complete inversion of solvent spin a. The curves on the graphs are generated by the use of a full 6×6 relaxation matrix, a truncated CSSR 4×4 matrix, a truncated ERF-type 3×3 matrix (dashed line), and a 3×3 matrix with no intermolecular contributions (dotted line). Under no circumstances were the first two curves visually discernible for the considered molecular model, so that both are depicted with a continuous line.

molecular NOE near its maximum value (the heteronuclear NOE in AX remains positive). The A proton is subject to a hard pulse in this simulated experiment (figure 4(*a–c*)), or soft pulse which selectively inverts one of doublet lines and gives rise to v_1 and v_3 (figure 4(*d–f*)). The same pulse leads to the partial excitation of the solvent spins. This models the situation where a multiline (possibly broadened) solvent spectrum is affected by an RF pulse applied to the solute spins. It is assumed that v_4 is excited to one half of its maximum possible amplitude and v_6 to its maximum (which implies that of the two solvent spins a is inverted). Molar composition of the mixture used in the simulations of figure 4 is 1 : 100. Rotational correlation times are set at 1/9 of self-diffusion correlation times in compliance with hydrodynamic relationships. Intermolecular contributions account for 37% of the proton A self-relaxation rate under these conditions, which is realistic for small molecules [41, 42].

The curves from exact and CSSR approaches cannot be distinguished visually in figure 4, while the ERF curve is considerably off target. This correlates well with the fact that $\mu_1^{[14]}$ transfer at 8% and 16% is two orders of magnitude higher than $\mu_1^{[16]}$. The ERF curve is based on true values of dipolar relaxation elements (equations (3) and (8)). If these elements are treated as fitting parameters, as is usually done, ERF curves can be brought into good agreement with exact ones. However, in doing so ERF coefficients are moved far apart from prototype dipolar elements. This can be seen especially clearly from the $v_1(t)$ plot in figure 4(*d*), where it appears preferable to ignore intermolecular interactions rather than to use genuine dipolar relaxation rates in the role of ERF terms. Note also that neglecting $\mu_1^{[14]}$ results in steeper relaxation decay in conditions of negative NOE.

Standard fitting procedures yield the ERF terms that may differ significantly from original dipolar contributions. This effect is frequency dependent as intermolecular NOE transfer varies with frequency. This effect appears only when the solvent is perturbed by RF pulses, since the influence of intermolecular NOE is minimal when the solvent remains unaffected (conversely, intermolecular NOE can be removed by decoupling of the solvent over the period of relaxation measurements). In these circumstances one should exercise caution in interpreting ERF relaxation rates. For example, the attempt to compare ERF contributions obtained from measurements in hydrogenated solvents with those found in deuterated solvents can be compromised, and the result can be different from what is expected based on gyromagnetic ratios [19–22]. While the ERF model is likely to recover genuine dipolar terms in the case of a deuterated solvent, which is not affected by RF pulses, the same may not be true for a protic solvent, as demonstrated by figure 4.

A situation similar to that illustrated in figure 4 is observed also in the fast and intermediate motion regimes, as CSSR invariably shows perfect agreement with exact results while ERF curves are found occasionally to deviate. The transfer coefficient $\mu_1^{[16]}$ stays at least one order of magnitude below $\mu_1^{[14]}$, and always is found well below the level where it can influence the shape of curves.

As discussed previously, $\mu_1^{[16]}$ tends to be averaged out in the extreme narrowing limit as a and b effectively take central positions in rapidly rotating molecules. Even if rotation and translation proceed on the same time scale the intermolecular transfer $\mu_1^{[16]}$ is undercut since intramolecular relaxation prevails in these conditions. Similarly, in the slow motion limit the relaxation of the solvent is dominated by intramolecular proton–proton interactions leading to large increases in R_{66} (through the spectral density at zero frequency). Increases in R_{66}, combined with declines of R_{11}, are detrimental for $\mu_1^{[16]}$ for the reasons that can be deduced from first-order perturbation theory: small off-diagonal element R_{16} fails to couple two levels that are set wide apart.

If we recall that this test has been devised in such a way as to provide for a maximum $\mu_1^{[16]}$, in particular using the ab molecule with exaggerated difference in spin eccentricities, we are led to believe that the results are quite conclusive and $\mu_1^{[16]}$ transfer can safely be neglected. The CSSR approximation is found to be sound in this respect.

However, this test is not conclusive as far as relaxation coupling within the solvent is concerned, since the system in question displays little of this effect. It is worth noting that if ab relaxes solely through an intramolecular DD mechanism, then our choice of modes provides for monoexponential $v_4(t)$. Feeble effects of coupled relaxation in the solvent arise from intermolecular DD interactions. They manifest themselves through weak $\mu_4^{[46]}$ transfer (tables 1 and 2) which has the same structure as $\mu_1^{[16]}$, also depends on difference in eccentricities, and, similarly, can be neglected. It has been confirmed experimentally [43] that the pure AB spectrum shows simple exponential recovery if external relaxation at A and B sites is the same. We shall now discuss the possibilities for more pronounced coupled relaxation effects in the solvent.

As first-order relaxation mechanisms are taken into account, they may contribute modestly to $\mu_4^{[46]}$ and $\mu_4^{[45]}$ through cross-correlation with DD interaction (CSA-DD cross-correlation is the only example). Autocorrelations also contribute to $\mu_4^{[46]}$, but a and b terms appear with different signs, so that is expected

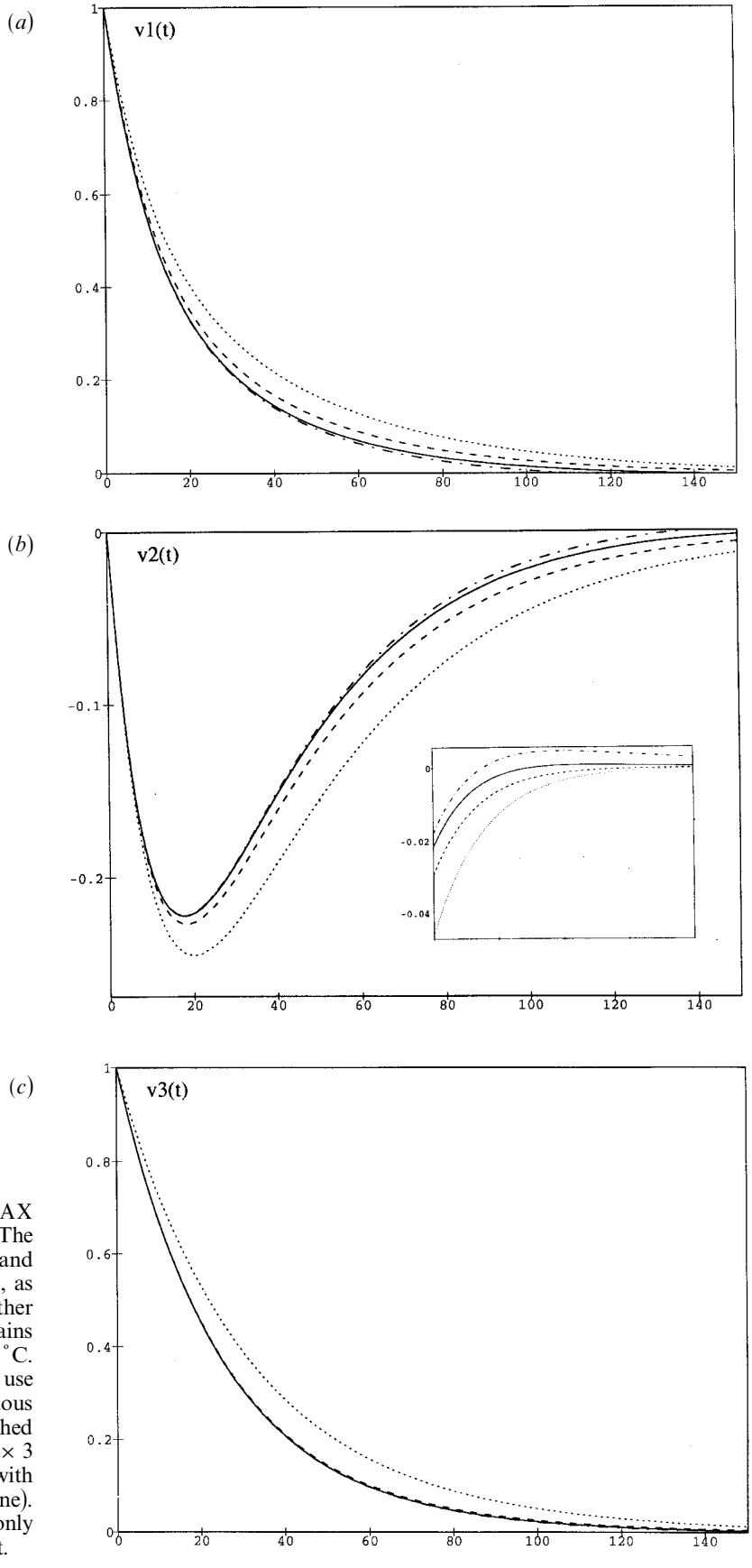

Figure 5. Relaxation profiles $v_1(t)$–$v_3(t)$ for an AX spin system interacting with an abx solvent. The model system is based on the geometry and dynamics of $^{13}CHCl_3$ dissolved in $^{13}C^{12}CH_2$, as deduced from NMR measurements and other sources [46]. The model mixture contains 1 mol% chloroform at a temperature − 54 °C. The curves on the graphs are generated by use of a full 10×10 relaxation matrix (continuous line), a truncated CSSR 4×4 matrix (dashed and dotted line), a truncated ERF-type 3×3 matrix (dashed line), and a 3×3 matrix with no intermolecular contributions (dotted line). The first two curves can be distinguished only in the area of the tails, as shown in the inset.

to be insignificant. At the same time, the magnitude of $\mu_4^{[46]}$ can be boosted by introducing a third spin, x, in the solvent spin system, and this led us to examine the case of an abx-type solvent. Relaxation coupling between the solvent modes is determined in this situation by a difference in ax and bx dipolar relaxation rates, which can be large if x is located close to a and far away from b in a solvent molecule. This is in contrast to similar intermolecular terms (table 3) where the difference is evened out by molecular motion. It is the presence of a third spin that determines the complex nature of relaxation in ab spectra [44, 45].

The AX–abx mixture used in simulations was modelled after a solution of $^{13}CHCl_3$ chloroform in $^{13}C^{12}CH_2$ acetylene. All relevant structural and dynamical parameters can be found in the literature [46]. Acetylene spins are coupled with $J_{ab} = 9{\cdot}5$ Hz, $J_{ax} = 249$ Hz, $J_{bx} = 50$ Hz, and $\omega_a - \omega_b$ is vanishingly small. Initial conditions are based on selective inversion of the low-field line in the A doublet which produces equal amounts of $v_1(0)$ and $v_3(0)$. Excitation of the solvent is modelled using a 180° rectangular pulse which falls on-resonance with ω_a. Following the pulse, spin states are computed numerically in the direct product basis and then converted into the operator basis (equation (16)). All of the modes v_4, v_6, and v_7 are excited efficiently. Intermolecular relaxation is found to contribute a reasonable 11% to the A self-relaxation rate. The model of motion adopted here does not capture fine details of motion such as rotational anisotropy or long-time tails of rotational correlation functions [47].

The simulated system is in the fast motion regime with $\omega\tau_{transl}^{AXabx} = 0{\cdot}086$. In conditions of positive intermolecular NOE relaxation profiles display the same pattern as seen previously for negative intermolecular transfer. Only microscopic differences between exact and CSSR curves can be spotted (figure 5), being the result of two-step transfer with $\mu_4^{[46]}$, $\mu_4^{[47]} = 8\%$ and $\mu_1^{[14]} = 2\%$ (or, more rigorously, the result of mixing within the exact 10×10 relaxation matrix).

In subsequent simulations, motional parameters of the model have been varied, covering a multitude of points in both slow and fast motion domains. The CSSR and exact curves were found to be in very good agreement, with rare discrepancies on the same small scale as seen in figure 5. This result suggests strongly that the complex chateracter of solvent relaxation can be ignored as long as the study concentrates on solute relaxation. The transfer $\mu_4^{[46]}$, $\mu_4^{[47]}$ of course cannot be neglected in studying selective relaxation of abx. However, it has relatively little effect on effective decay rate of Q_4 and consequently minor influence on AX relaxation.

Optimization techniques could have been employed to find the maximum deviation in the CSSR curves. However, the effect itself is too subtle, the number of fitting parameters too large (this includes the variety of initial conditions and spin configurations), and constraints too vague (such as maintaining reasonable proportion of intra- and intermolecular rates) to justify the use of optimization methods.

The curves generated on the basis of an exact relaxation matrix were used as computer simulated data in order to estimate the quality of the ERF interpretation. The results are to be reported elsewhere. We would indicate here only that in the situation when the solvent spin reservoir is perturbed by RF pulses, ERF provides an imprecise measure of intermolecular DD contributions, and may even cause errors in the determination of intramolecular parameters, such as τ_{rot}, if external relaxation is sufficiently strong. For example, ERF-based fitting procedure, as applied to the set of simulated curves 5(*a–c*), underestimates the proton CSA by 80% (fits are not shown on the plot). Use of the CSSR approach can be recommended in certain cases to improve the analysis of experimental data. The example of such a practical application can be found in our previous work [17].

One other problem that is well suited to benefit from the application of the CSSR approach is cross-relaxation between molecular groups. Recent study of relaxation between methylene groups in a hydrocarbon chain [48] demonstrates the breakdown of the ERF model, failing to reproduce the spectral densities within a methylene group, and yielding negative values for certain ERF rates. Only intramolecular correlation functions are needed in this situation, and CSSR has a good chance of providing consistent interpretation.

The help of T. R. J. Dinesen in the preparation of this manuscript is gratefully acknowledged, and we thank the referees for helpful comments.

References

[1] Wüthrich, K., 1986, *NMR of Proteins and Nucleic Acids* (New York: Wiley).
[2] Blackledge, M. J., Brüschweiler, R., Griesinger, C., Schmidt, J. M., Xu Ping, and Ernst, R. R., 1993, *Biochemistry*, **32,** 10960.
[3] Clore, G. M., and Gronenborn, A. M., 1983, *J. magn. Reson.*, **53,** 423.
[4] Goldman, M., 1984, *J. magn. Reson.*, **60,** 437.
[5] Grant, D. M., Mayne, C. L., Liu, F., and Xiang, T.-X., 1991, *Chem. Rev.*, **91,** 1591.
[6] Sørensen, O. W., Eich, G. W., Levitt, M. H., Bodenhausen, G., and Ernst, R. R., 1983, *Progr. NMR Spectrosc.*, **16,** 163.
[7] Khazanovich, T. N., and Zitserman, V., 1971, *Molec. Phys.*, **21,** 65.

[8] Krishna, R. N., and Gordon, S. L., 1973, *J. chem. Phys.*, **58,** 5687.
[9] Mackor, E. L., and MacLean, C., 1965, *J. chem. Phys.*, **42,** 424; 1966, *J. chem. Phys.*, **44,** 2708.
[10] Solomon, I., 1955, *Phys. Rev.*, **99,** 559.
[11] Abragam, A., 1961, *The Principles of Nuclear Magnetism* (Oxford: Clarendon Press).
[12] Hwang, L. P., and Freed, J. H., 1975, *J. chem. Phys.*, **63,** 4017.
[13] Ayant, Y., Belorizky, E., Alizon, J., and Gallice, J., 1975, *J. Phys.*, **36,** 991.
[14] Ayant, Y., Belorizky, E., Fries, P., and Rosset, J., 1977, *J. Phys.*, **38,** 325.
[15] Westlund, P.-O., and Lynden-Bell, R. M., 1987, *J. magn. Reson.*, **72,** 522.
[16] Odelius, M., Laaksonen, A., Levitt, M. H., and Kowalewski, J., 1993, *J. magn. Reson.* A, **105,** 289.
[17] Khazanovich, T. N., and Skrynnikov, N. R., 1995, *J. phys. Soc. Jap.*, **64,** 631. Given normalization of equation (1) in this work, equation (4) should read $W_{41} = n_2 W_{14}/n_1$. The results remain unaffected.
[18] Courtieu, J. M., Mayne, C. L., and Grant, D. M., 1977, *J. chem. Phys.*, **66,** 2669.
[19] Chenon, M. T., Bernassau, J. M., and Coupry, C., 1985, *Molec. Phys.*, **54,** 277.
[20] Courtieu, J., Jullien, J., Lai, N. T., Guillois, A., Gonord, P., Kan, S. K., and Mayne, C. L., 1980, *J. chem. Phys.*, **72,** 953.
[21] Fuson, M. M., and Prestegard, J. H., 1982, *J. chem. Phys.*, **76,** 1539.
[22] Foucat, L., Chenon, M. T., and Werbelow, L., 1990, *J. phys. Chem.*, **94,** 5791.
[23] Brüschweiler, R., and Wright, P. E., 1994, *Chem. Phys. Lett.*, **229,** 75.
[24] Otting, G., and Liepinsh, E., 1995, *Accounts chem. Res.*, **28,** 171.
[25] Halle, B., 1984, *Molec. Phys.*, **53,** 1427.
[26] Denisov, V. P., and Halle, B., 1994, *J. Amer. chem. Soc.*, **116,** 10324.
[27] Kay, L. E., Nicholson, L. K., Delaglio, F., Bax, A., and Torchia, D. A., 1993, *J. magn. Reson.*, **97,** 359.
[28] Ernst, R. R., Bodenhausen, G., and Wokaun, A., 1987, *Principles of Nuclear Magnetic Resonance in One and Two Dimensions* (Oxford: Clarendon Press).
[29] Sinivee, V., 1972, *J. magn. Reson.*, **7,** 127.
[30] Alla, M., and Lippmaa, E., 1971, *J. magn. Reson.*, **4,** 241.
[31] Skrynnikov, N. R., unpublished.
[32] He, Q., Richter, W., Vathayam, S., and Warren, W. S., 1993, *J. chem. Phys.*, **98,** 6779.
[33] Jeener, J., Vlassenbroek, A., and Broekaert, P., 1995, *J. chem. Phys.*, **103,** 1309.
[34] Canet, D., 1989, *Progr. NMR Spectrosc.*, **21,** 237.
[35] Vold, R. R., and Vold, R. L., 1978, *Progr. NMR Spectrosc.*, **12,** 79.
[36] Hubbard, P. S., 1963, *Phys. Rev.*, **131,** 275.
[37] Hubbard, P. S., 1969, *Phys. Rev.*, **180,** 319.
[38] Werbelow, L. G., and Grant, D. M., 1977, *Adv. magn. Reson.*, **9,** 189.
[39] Lipari, G., and Szabo, A., 1982, *J. Amer. chem. Soc.*, **104,** 4546.
[40] Macura, S., and Ernst, R. R., 1980, *Molec. Phys.*, **41,** 95.
[41] Smith, G. R., and Ternai, B., 1983, *Aust. J. Chem.*, **36,** 2227.
[42] Homer, J., and Valdivieso Cedeño, E. R., 1984, *J. chem. Soc. Faraday Trans.* 2, **80,** 375.
[43] Freeman, R., Wittekoek, S., and Ernst, R. R., 1970. *J. chem. Phys.*, **52,** 1529.
[44] Vold, R. L., and Vold, R. R., 1974, *J. chem. Phys.*, **61,** 2525.
[45] Bain, A. D., Hughes, S. G., and Hamer, G. K., 1992, *J. magn. Reson.*, **96,** 613.
[46] Mourits, F. M., and Rummens, F. H. A., 1977, *Can. J. Chem.*, **55,** 3007; Scheie, C. E., Peterson, E. M., and O'Reilly, D. E., 1973, *J. chem. Phys.*, **59,** 2303; Mohanty, S., 1973, *Chem. Phys. Lett.*, **18,** 581; Bender, H. J., and Zeidler, M. D., 1971, *Ber. Bunsenges. phys. Chem.*, **75,** 236; Dinesh and Rogers, M. T., 1972, *J. chem. Phys.*, **56,** 542; Bhattacharyya, P. K., and Dailey, B. P., 1973, *J. magn. Reson.*, **12,** 36; *CRC Handbook of Chemistry and Physics*, 76th Edn., 1995 (Boca Raton; FL: CRC Press).
[47] Tironi, I. G., and van Gunsteren, W. F., 1994, *Molec. Phys.*, **83,** 381.
[48] Fuson, M. M., and Belu, A. M., 1994, *J. magn. Reson.* A, **107,** 1.